Numerical Heat Transfer, Part A, 66: 17–40, 2014

ISSN: 1040-7782 print/1521-0634 online
DOI: 10.1080/10407782.2013.869081

Taylor & Francis
Taylor & Francis Group

OPTIMAL POSITIONING OF STRIPS FOR HEAT TRANSFER REDUCTION WITHIN AN ENCLOSURE

A. Haghighi and K. Vafai
Department of Mechanical Engineering, University of California, Riverside, Riverside, CA, USA

Heat transfer reduction capabilities of a vertical or a horizontal adiabatic partial partition fixed in a differentially heated cavity with insulated top and bottom walls are analyzed and compared. The effects of length and location of the partition is taken into account for aspect ratios from 1 to 4 and for Rayleigh numbers from 10^3 to 10^6. Different characteristics of square and higher aspect ratio cavities are compared and a comprehensive correlation of the heat transfer reduction is introduced, incorporating all the pertinent parameters. Based on our results, vertical baffles more efficiently reduce heat transfer, in most cases.

1. INTRODUCTION

Natural convection heat transfer through air filled cavities of different geometries is a classical problem which has received a great deal of attention, due to its special theoretical and practical importance. This problem has a wide variety of engineering applications including cooling electronics devices, designing heat exchangers and solar thermal collectors, heating and ventilating applications, and energy conservation in refrigeration units. Comprehensive reviews on the subject have been written by Catton [1], Ostrach [2], and Jaluria [3]. In many applications obstructions of different shapes and orientations are fixed in the enclosure with the main purpose of adjusting the flow and heat transfer characteristics of the cavity, by modifying the flow and temperature fields of the system [4–31].

Various wall and partition conditions have been investigated in the literature numerically [5–15]. Zimmerman and Acharya [12] presented a numerical simulation of natural convection in a square cavity with perfectly conducting horizontal walls, and with conductive dividers. They accounted for the effects of thickness and conductivity of the baffle. Frederick et al. [13] studied the same problem with a partition at the center of the hot wall and investigated the effect of partitions length and conductivity. Acharya and Jetli [14] extended this work by taking into consideration the effects of the location and height of the partition and also end

Received 15 August 2013; accepted 30 September 2013.
Address correspondence to K. Vafai, University of California, Riverside, Department of Mechanical Engineering, A3103 Bourns Hall, Riverside, CA 92521, USA. E-mail: vafai@engr.ucr.edu
Color versions of one or more of the figures in the article can be found online at www.tandfonline.com/unht.

NOMENCLATURE

A	aspect ratio, $(= H/W)$	T'	local temperature, K
D_x	location of vertical partition, $(= x/W)$	t	dimensionless thickness of partition
D'_x	dimensional distance of vertical partition from the left wall	t'	thickness of partition, m
		u, v	dimensionless velocity components
D_y	location of horizontal partition, $(= y/H)$	u', v'	local velocity components
D'_y	dimensional distance of horizontal partition from the bottom wall	W	width of enclosure, m
		x', y'	dimensional Cartesian coordinates
g	gravitational acceleration, m/s^2	x, y	dimensionless Cartesian coordinates, $(= x'/W, y'/H)$
H	height of enclosure, m	**Greek Symbols**	
h	local heat transfer coefficient, W/m^2K	α	thermal diffusivity coefficient, m^2/s
k	thermal conductivity, W/mK	β	thermal expansion coefficient, $1/K$
L	dimensionless length of partition, $(= L'/H \text{or} L'/W)$	ν	momentum diffusivity of fluid, m^2/s
		ρ	density of the fluid, kg/m^3
L'	length of partition, m	ψ	dimensionless streamfunction
Nu	local Nusselt number	ψ'	dimensional streamfunction
$\overline{\text{Nu}}$	average Nusselt number	**Subscripts**	
Pr	Prandtl number	C	cold wall
p'	local pressure, N/m^2	H	hot wall
p	dimensionless pressure	min	minimum
Ra	Rayleigh number	p	partition
R_r	Nusselt number reduction ratio		
T	dimensionless temperature		

wall conditions on the heat transfer characteristics of the enclosure. Chen and Ko [15] presented a numerical study for the case of a rectangular enclosure, with $A = 2$ and a partition ratio of $1/2$ with an opening, in which two side walls were maintained at uniform heat flux condition and the top and bottom walls were insulated. They observed that the partition opening, rather than the conductivity, significantly influences the overall heat transfer.

Nag et al. [16] investigated the effect of a horizontal thin plate with infinite or zero thermal conductivity, positioned on the hot wall of the square cavity while length and location of the partition were variable. They reported that an adiabatic partition reduced heat transfer especially when located close to the ceiling, due to blocking the convection currents. Shi and Khodadadi [17] and Tasnim and Collins [18] studied the same problem in more detail, using different numerical techniques and focused only on perfectly conducting partitions. They have reported that perfectly conducting partition increased the heat transfer due to fin's enhanced heating of the baffle, while the baffles disturbing the flow patterns had a decreasing effect. Also Xi and khodadadi proposed correlations of Nusselt number with regards to parameters studied for the specific case of perfectly conducting partitions. Later, Bilgen [19] numerically studied the same problem by considering strip to air conductivity values ranging from 0 to 60. For a completely adiabatic partition, he reported that at low Rayleigh numbers, a strip located close to the center yields maximum decrease in average Nusselt number. Moreover, he reported that longer conductive partitions have a more remarkable effect on the flow field and heat transfer inside the cavity.

Oosthuizen and Paul [20] studied natural convection in rectangular cavities with aspect ratios between 3 and 7, with a horizontal plate at the center of the cold

wall. They reported an increase in heat transfer due to the presence of adiabatic or perfectly conducting partitions on the cold wall. The effect of placing an array of horizontal partitions on the hot or cold walls, has been investigated [21–25]. Scozia and Frederick [21] considered slender cavities of $A = 20$ and taller, with multiple inclined conducting strips on the cold wall reported longer strips yielding lower average Nusselt numbers. They also reported that as the inter fin aspect ratio was varied from 20 to 0.25 and therefore number of fins increases, specific locations for the strip resulted in maximum or minimum values of mean Nusselt number, at different Rayleigh numbers. Facas [22] numerically studied the effect of conducting baffles length and orientation, when fixed on the hot and cold walls of a narrow cavity with adiabatic horizontal walls. He studied implementing a single baffle as one of the limiting cases in his studies and reported existence of multicellular flow for a non-dimensional baffle length of 0.1, which breaks down into secondary circulations for the baffle length equal to 0.3 or greater, for the specific case of height to width ratio equal to 15. Terekhov and Terekhov [24] considered the case of multiple adiabatic or infinitely heat conducting horizontal partitions mounted on the hot wall of a cavity with adiabatic horizontal walls for an aspect ratio of 35. They found that for adiabatic strips, there is an optimum number which can yield the lowest average heat transfer.

Bilgen [26] studied natural convection in cavities with height to width ratios of 0.3 to 0.4, when one or two conductive partial partitions are placed at two different positions on the adiabatic horizontal walls. Nowak and Novak [27] examined natural convection heat transfer in slender rectangular cavities of aspect ratios higher than 15, equipped with two small vertical partitions, located in the middle of horizontal walls. They reported two small vertical partitions of the same length, made of glass and located in the mid-plane of the cavity may reduce mean Nusselt number by up to six percent. These works have carried out studies on vertical partitions with infinite or finite thermal conductivities. Oztuna [28] examined an enclosure with a conductive vertical partition fixed on the bottom wall, for $\mathrm{Ra} = 10^4, 10^5,$ and 10^6. He reported that as the partition's distance from the hot wall increases, the average Nusselt number first decreases to a minimum and then increases for low Ra, while for high Ra, it first increases to a maximum and then decreases.

For cases with adiabatic partial partitions, Ciofalo et al. [29] have investigated the influence of various boundary conditions at the end walls and the partitions including adiabatic condition, when two symmetrical finitely thick partitions are extended from the center of upper and bottom walls for aspect ratios from 0.5 to 10. They have reported that the efficiency of partitions depends on Rayleigh number and aspect ratio, as well as partitions height in a complex way and is greatest for low Rayleigh numbers and high aspect ratios. Nansteel and Grief [30] performed an experimental study considering a partition suspended from the upper wall of a shallow cavity filled with water, for $\mathrm{Ra} = 10^{10}$ to 10^{11}. Hanjalic et al. [11] studied the same turbulent problem numerically for Rayleigh number range of $10^{10} - 10^{12}$, and considered shallow cavities with an adiabatic partition at the center of the upper wall. Recently Ilis et al. [31] studied heat transfer reduction in square cavities, due to an adiabatic barrier fixed on the upper wall. They considered lengths up to one half of enclosure's height, and accounted for the effects of length and location of the partitions and reported that heat transfer reduction effectiveness depends on length and location of the adiabatic barrier and the Rayleigh number.

Our literature search has revealed that a comprehensive investigation of heat reduction capabilities of a single adiabatic horizontal partition, placed on either hot or cold wall has not been performed yet. Most of the previous studies have carried out studies on partitions with either infinite or finite thermal conductivities. Additionally, works on adiabatic partial partitions, have mostly either performed turbulent studies or have considered slender cavities of very high aspect ratio enclosures, in which some discussed applying a single adiabatic partition only as one of the limiting cases. They have not analyzed how increasing aspect ratio from $A = 1$ (square enclosure) to higher aspect ratio cases contributes to the evolution of multicellular flows, when horizontal partitions are used. Besides, effects of implementing a vertical partition in a higher aspect ratio enclosure, has not been considered in detail. Furthermore, comparisons between the effectiveness of horizontal and vertical partial partitions respectively mounted on the side or end walls for square and higher aspect ratio cavities needs to be studied.

In the present work, we will study and compare vertical and horizontal adiabatic partial partitions in differentially heated rectangular cavities with insulated horizontal walls. The effects of length and location of the baffle will be taken into account for Rayleigh numbers from 10^3 to 10^6, with the main objective of determining how the parameters involved, could bring about maximum heat transfer depression across the system. The investigation is performed for square enclosures, as well as cavities with higher aspect ratios up to $A = 4$ and the computed data is correlated for all cases studied.

2. PROBLEM DEFINITION AND ASSUMPTIONS

A schematic drawing of the enclosure, the two types of partitions under consideration, the boundary conditions and the coordinate system utilized in the present study is illustrated in Figure 1. Height and width of the enclosure are, respectively, designated by H and W, and A is defined as the aspect ratio ($A = H/W$). The length of the geometry perpendicular to the plane of the figure is assumed to be long; therefore the problem is considered to be two dimensional. The enclosure is perfectly insulated on the top and bottom walls while there is a temperature gradient between the left and right walls which are respectively maintained at constant temperatures T_H and T_C, with $T_H > T_C$. A partition with length L' is fixed either on the sidewalls or on the top or bottom walls, and is assumed to have negligible thickness and thermal conductivity. The dimensionless length of the partition is defined as $L = L'/H$ for vertical partitions and as $L = L'/W$ for horizontal partitions. The distance from the hot wall to the vertical partition is designated as D'_x and the distance from the bottom wall to the horizontal partition as D'_y, which are referred to as the location of the partition. Dimensionless locations of vertical and horizontal partitions are defined as $D_x = D'_x/W$ and $D_y = D'_y/H$, respectively.

The working fluid in the domain is air which is considered to be Newtonian and incompressible with Pr= 0.71. Gravitational body forces in negative y direction act on the air present in the domain in which there are density gradients caused by the different temperatures of the sidewalls. The outcome is a buoyancy force which causes clock wise circular convection currents of the fluid in the enclosure. The air enclosed in the cavity is considered to have homogeneous thermophysical properties

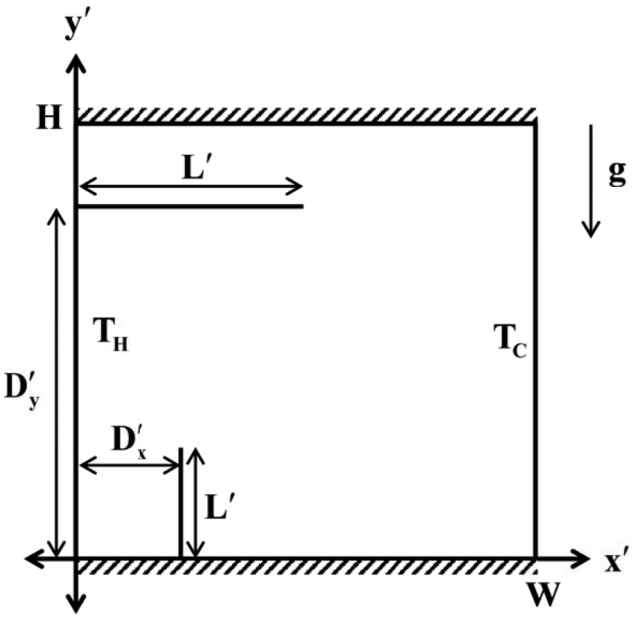

Figure 1. Schematic of the enclosure studied in the present work, along with representative vertical and horizontal partial partitions.

except for density, which is determined by the Boussinesq approximation. Rayleigh number varies from 10^3 to 10^6. In this range, the flow is completely laminar and both conduction and free convetion contribute to the overall heat transfer of the system, with convection playing progressively a more important role as Ra increases. Heat transfer by radiation is considered to be insignificant and it is assumed that there is no viscous dissipation or thermal energy generation in the system.

3. GOVERNING EQUATIONS AND BOUNDARY CONDITIONS

Governing equations can be normalized by defining the following dimensionless parameters.

$$x \equiv \frac{x'}{W}, \quad y \equiv \frac{y'}{H}, \quad u \equiv \frac{u'W}{\alpha}, \quad v \equiv \frac{v'H}{\alpha}, \quad T \equiv \frac{T' - T_C}{T_H - T_C}, \quad p \equiv \frac{p'H^2}{\rho\alpha^2} \tag{1}$$

Parameters x and y are nondimensional distances in the two perpendicular directions of the coordinate system. Variables u' and v' are local dimensional velocity components in the x and y directions; and T',p' are local values of temperature and pressure in the domain. Variables u, v, T, and p are equivalent nondimensional properties of the problem. In addition, α is the thermal diffusivity coefficient and ρ is the density of the fluid. Based on the assumptions provided and the nondimensional parameters introduced, dimensionless continuity, momentum and energy equations can be written as follows.

$$\frac{\partial u}{\partial x} + \frac{\partial v}{\partial y} = 0 \tag{2}$$

$$u\frac{\partial u}{\partial x} + v\frac{\partial u}{\partial y} = -\frac{\partial p}{\partial x} + \mathrm{Pr}\left(\frac{\partial^2 u}{\partial x^2} + \frac{\partial^2 u}{\partial y^2}\right) \tag{3}$$

$$u\frac{\partial v}{\partial x} + v\frac{\partial v}{\partial y} = -\frac{\partial p}{\partial y} + \mathrm{RaPr}T + \mathrm{Pr}\left(\frac{\partial^2 v}{\partial x^2} + \frac{\partial^2 v}{\partial y^2}\right) \tag{4}$$

$$u\frac{\partial T}{\partial x} + v\frac{\partial T}{\partial y} = \frac{\partial^2 T}{\partial x^2} + \frac{\partial^2 T}{\partial y^2} \tag{5}$$

where $\mathrm{Pr} \equiv \nu/\alpha$ and $\mathrm{Ra} \equiv g\beta(T_H - T_C)W^3/\alpha\nu$, β is coefficient of thermal expansion, and ν is the momentum diffusivity of the working fluid. Boundary conditions are comprised of no slip conditions on all boundaries and the partition, along with isothermal conditions on the sidewalls and adiabatic conditions on the partition, and top and bottom walls.

$u = v = 0$ and $T = 1$ on the hot wall
$u = v = 0$ and $T = 0$ on the cold wall
$u = v = 0$ and $\partial T/\partial y = 0$ on the top and bottom walls
$u = v = 0$, plus $\partial T/\partial y = 0$ or $\partial T/\partial x = 0$, respectively, on the horizontal and vertical partition (6)

Nusselt number value at any point on the hot wall and the average Nusselt number over the hot wall can be calculated as follows.

$$\mathrm{Nu} \equiv \frac{hL}{k} = -\left.\frac{\partial T}{\partial x}\right|_{x=0}, \quad \overline{\mathrm{Nu}} \equiv \left.\int_{y=0}^{1} \frac{\partial T}{\partial x}\,dy\right|_{x=0} \tag{7}$$

Where h is the heat transfer coefficient, and k is the thermal conductivity. $\overline{\mathrm{Nu}}$ provides a measure of the total heat flux through the enclosure. When barriers are implemented, Nusselt number reduction ratio which represents the heat flux adjustments caused by the partitions is introduced as the ratio of $\overline{\mathrm{Nu}}$ when the barrier is mounted, to the $\overline{\mathrm{Nu}}$ in the absence of partitions,

$$R_r = \frac{\overline{\mathrm{Nu}}_{\text{in the presence of partitions}}}{\overline{\mathrm{Nu}}_{\text{in the absence of partitions}}} \tag{8}$$

By defining nondimensional stream function as $\psi = \psi'/\alpha$, the normalized stream function values are calculated from the following.

$$u = \frac{\partial \psi}{\partial y}, \quad v = -\frac{\partial \psi}{\partial x} \tag{9}$$

4. NUMERICAL SOLUTION

In the absence of partitions, velocity and temperature fields have a point reflection symmetry through the center point of the cavity, due to the geometry and the boundary conditions configuration of the problem. This symmetry can be visually inspected in Figure 2*a* which presents streamlines and isotherms in

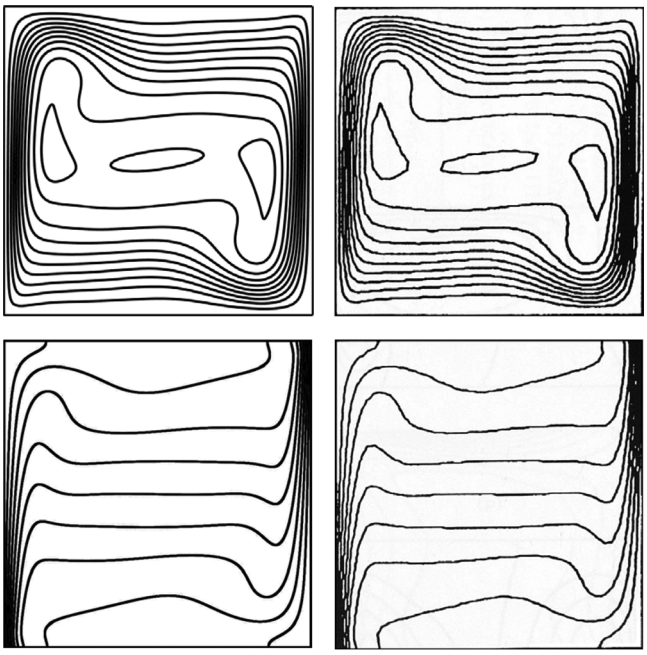

Figure 2. Streamlines ($\psi : -16.27,\ -15.07(1.675)0$) and isotherms ($T : 0(0.1)1$) for $\mathrm{Ra} = 10^6$ in the absence of partitions. (*a*) Present work, and (*b*) results from de Vahl Davis [32].

the specific case of a square cavity filled with air at $\mathrm{Ra} = 10^6$. As such, only vertical and horizontal partitions, respectively, fixed on the bottom and left wall are studied here, knowing that their reflected equivalents through the center point of the cavity, fixed on the other two walls would yield similar results. A range of Rayleigh numbers from 10^3 to 10^6 are considered and the problem is solved for enclosures with four different aspect ratios, $A = 1, 2, 3,$ and 4 with a vertical or a horizontal partition mounted with three different values for the non-dimensional length, $L = 0.25, 0.5,$ and 0.75, and four different values for the nondimensional location, $D_{x \text{ or } y} = 0.2, 0.4, 0.6,$ and 0.8. COMSOL Multiphysics software is used to solve the problem numerically, by means of finite element method. The PARDISO solver package in this program is set to directly solve the large sparse linear system of equations resulting from the governing partial differential equations (Eqs. (2)–(5)) in the discretized computational domain, with less than 10^{-4} relative error. The velocity and temperature fields are obtained and their contour profiles are plotted. Accordingly, the average Nusselt number ($\overline{\mathrm{Nu}}$) on the hot wall and stream function values of the streamlines are calculated based on Eqs. (7) and (9), respectively.

4.1. Grid Independence Studies

The triangular mesh used in the present study has a non-uniformly distributed grid size, with a larger concentration on the walls and the partition compared

Table 1. Grid independence study, specifying different mesh distributions that were experimented within this work

Mesh type	Maximum element size	Minimum element size	Maximum element growth rate	Resolution of curvature
1	0.045 (0.0280)	0.02 (0.0040)	1.15 (1.1)	0.30 (0.25)
2	0.035 (0.0130)	0.01 (0.0015)	1.13 (1.08)	0.30 (0.25)
3	0.028 (0.0067)	0.004 (0.0002)	1.10 (1.05)	0.25 (0.20)
4	0.013 (0.0067)	0.0015 (0.0002)	1.08 (1.05)	0.25 (0.20)

Numbers in parentheses are values at the boundaries and on the partition.

to other regions. The distribution is controlled by manipulating four quantitative parameters which are the maximum and minimum allowed element size, the maximum rate at which the element size can grow and the curvature resolution, for which a lower value gives a finer mesh along the boundaries. Four different types of triangular mesh with different grid sizes have been generated with mesh type 1 being the coursest and mesh type 4 being the finest. Specifications of each mesh type are presented in Table 1. By utilizing these four types of mesh, the computational domain for different cases studied in the prersent work are discretized to a number of triangular elements ranging roughly from 5×10^3 to 70×10^3.

At high Rayleigh numbers or when the partitions are mounted, finer mesh settings are required to achieve accurate results, due to increased complexity of the system. To confirm grid independence, a systematic set of computational runs were performed for all the cases studied. Due to wide variety of the situations being investigated, four different configurations of partial partitions in an air filled square enclosure with $\mathrm{Ra} = 10^6$ are chosen and presented here as a sample of the grid independence studies performed. Case (I) is in the absence of partitions while cases (II) and (III) are when a thin vertical or horizontal partition with ($L = 0.5$), is fixed in the middle of the bottom or the left wall, respectively. In case (IV), a vertical partition ($L = 0.25,\ D_x = 0.5$) and a horizontal partition ($L = 0.5,\ D_y = 0.5$) are fixed in the square cavity simultaneously. Figure 3 presents the grid independence

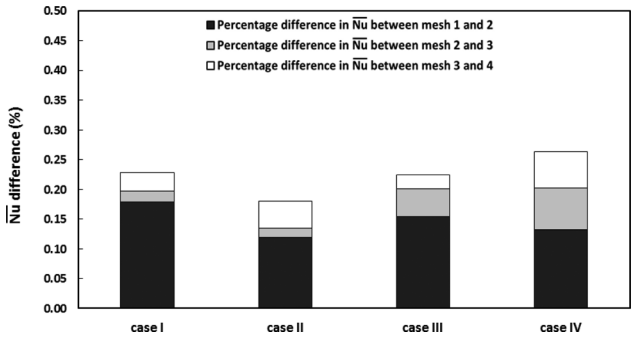

Figure 3. Effect of mesh concentration and grid independence study for $A = 1$ and $\mathrm{Ra} = 10^6$. case I: No partitions, case II: a vertical partition with $L = 0.5$, $D_x = 0.5$; and case III: a horizontal partition with $L = 0.5$, $D_y = 0.5$; and case IV: a vertical partition with $L = 0.25$, $D_x = 0.5$ and a horizontal partition with $L = 0.5$, $D_y = 0.5$.

Table 2. Effect of variations in the thickness of the partitions on $\overline{\mathrm{Nu}}$ and Nusselt reduction ratios for $\mathrm{Ra} = 10^6$ in the presence of a vertical partition ($L = 0.5,\ D_x = 0.5$)

Thickness	$\overline{\mathrm{Nu}}$	R_r	$\%_{\text{difference from t=0}}$
$t = 10^{-4}$	7.1786	0.8151	0.0032
$t = 10^{-3}$	7.1756	0.8148	0.0455
$t = 10^{-2}$	7.1295	0.8096	0.6866
$t = 2 \times 10^{-2}$	7.0968	0.8058	1.1421
$t = 5 \times 10^{-2}$	7.0028	0.7952	2.4515

study corresponding to the mesh types and the cases introduced. As can be seen, the differences between the $\overline{\mathrm{Nu}}$ resulting from any pair of the mesh types 2–4 are always less than 0.15% for any of the four cases. This establishes very good accuracy for these four mesh sizes which are used in the present study. Moreover, meshes 3 and 4 yield results less than 0.05% apart in any of four cases specified, and are used in most of the subsequent simulations.

4.2. Effect of Partitions Thickness

The partition's nondimensional thickness is defined as $t = t'/W$, where t' is the dimensional value of the thickness. In order to study the effect of t on the enclosure's heat transfer, a vertical partition with $L = 0.5$ and finite thickness is fixed at the middle of the bottom wall. Values of $\overline{\mathrm{Nu}}$ and R_r corresponding to this configuration at $\mathrm{Ra} = 10^6$ are summarized in Table 2 for different t values. Without any partitions the mean Nusselt would be $\overline{\mathrm{Nu}} = 8.8067$, and when a partition is applied with zero thickness, $\overline{\mathrm{Nu}} = 7.1788$. Table 2 shows that for thicknesses up to 2% of the width of the enclosure, results deviate less than 1.1% compared to the case when $t = 0$. Moreover real insulators have conductivities less than 0.1 W/(m.K). Considering this value for the conductivity of the partition yields $\overline{\mathrm{Nu}}$ values less than 0.15% apart for the case when $t = 2 \times 10^{-2}$ compared to when $t = 0$ and $k = 0$. Hence, in the present work the thickness and conductivity of partitions are assumed to be zero, knowing that produced results are applicaple to situations with finite partition thicknesses and material conductivities found in a real world setting.

5. VALIDATION OF THE NUMERICAL MODEL

For validation purposes, the computational results generated with our model are compared with the results available in the literature for an air filled square cavity differentially heated from the sides and insulated from the top and bottom. In Figures 2 and 4, the streamlines and isotherms obtained in the absence of partial partitions are compared with the results from de Vahl Davis [32] and Barakos et al. [33], at $\mathrm{Ra} = 10^6$ as the most crirtical situation. Additionally, in Table 3 mean Nusslet number values for $\mathrm{Ra} = 10^3$ to 10^6 are compared with the works of various authors. The results from this study are always less than 0.1% apart from the results of de Vahl Davis [32]. Table 3 and Figures 2 and 4 demonstrate excellent agreement between our results and previously published data.

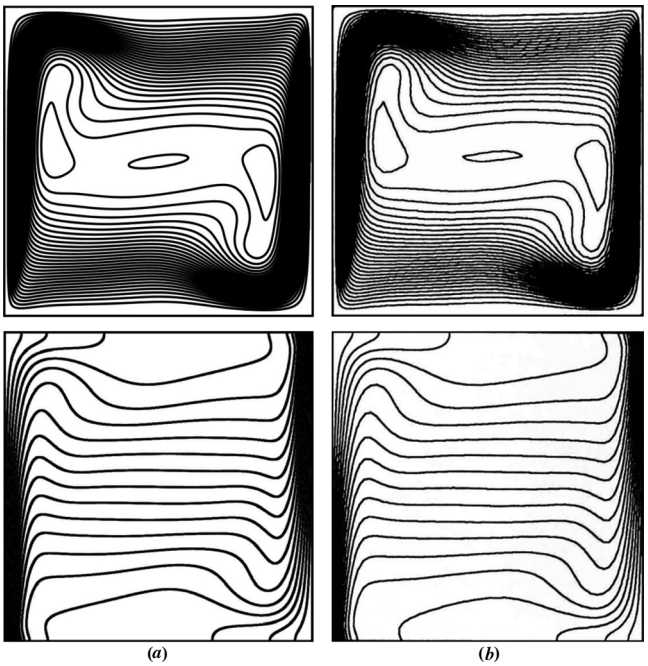

Figure 4. Streamlines ($\psi : 0(0.605)16.335$) and isotherms ($T : 0(0.05)1$) for $\mathrm{Ra} = 10^6$ in the absence of partitions, (*a*) Present work, and (*b*) results from Barakos et al. [33].

Furthermore, when a partial partition is mounted in the enclosure, our model is validated through comparisons with limited numerically obtained results accessible in the literatre. In Figure 5, an adiabatic partial partition with $L = 0.5$ is fixed on the top wall and at two different locations, and the generated streamlines and isotherms are compared with corresponding contour plots from Ilis et al. [31]. Also, some $\overline{\mathrm{Nu}}$ values are reported in Ilis et al. [31] for different configurations of a vertical partition fixed on the ceiling at various Rayleigh numbers which are compared with our result values in Table 4. For any specific set, the results are very close and the

Table 3. Comparison of mean Nusselt number ($\overline{\mathrm{Nu}}$) with previous works for an enclosure with no partitions

Reference	$\mathrm{Ra} = 10^3$	$\mathrm{Ra} = 10^4$	$\mathrm{Ra} = 10^5$	$\mathrm{Ra} = 10^6$
Fusegi et al. [35]	1.105	2.302	4.646	9.012
Shi and Khodadadi [17]	–	2.247	4.532	8.893
Markatos and Pericleous [34]	1.108	2.201	4.430	8.754
Bilgen [19]	–	2.245	4.521	8.800
Nag et al.[16]	1.12	2.24	4.51	8.82
Ilis et al. [31]	1.11	2.24	4.51	8.80
Barakos et al. [33]	1.114	2.245	4.510	8.806
de Vahl Davis [32]	1.118	2.243	4.519	8.799
Present Work	1.118	2.244	4.519	8.807

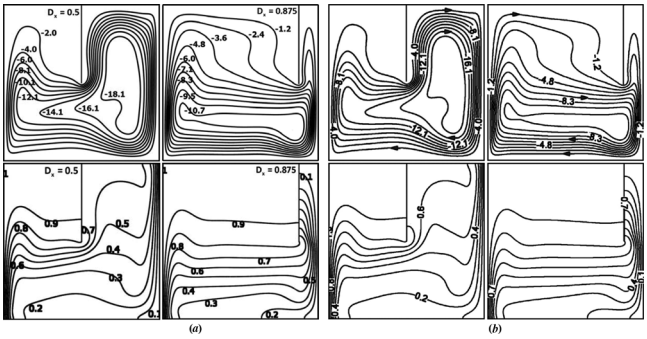

Figure 5. Streamlines and isotherms for $\mathrm{Ra} = 10^6$ in the presence of a vertical partition fixed on the top wall ($L = 0.5,\ D_x = 0.5,\ 0.875$). (*a*) Present work, and (*b*) results from Ilis et al. [31].

Table 4. Comparison of mean Nusselt number comparison with Ilis et al. [31] for an enclosure with a vertical partition mounted on the ceiling

Ra	L	D_x	R_r[31]	$R_{r\ \text{present work}}$	$\%_{\text{difference}}$
10^6	0.15	0.5	0.995	0.993	0.20
10^6	0.15	1.0	0.936	0.935	0.10
10^3	0.50	0.5	0.640	0.639	0.16
10^6	0.50	1.0	0.619	0.619	0.00
10^4	0.50	0.625	0.477	0.479	0.42
10^5	0.50	0.875	0.569	0.569	0.00

difference is less than 0.5%. Additionally, a diagram is presented in Ilis et al. [31] which depicts the variations of $\overline{\mathrm{Nu}}$ reduction ratio with regards to the location of the vertical barrier on the ceiling and at various Rayleigh numbers when $L = 0.5$. The same diagram is generated with the model employed in the present work, and is presented in Figure 6 along with the results from Ilis et al.'s [31] work. Excellent agreement can be seen in all the comparisons. In Figure 7*a*, a horizontal partition with $L = 0.7$ is mounted at the mid-height of the hotwall and its conductivity is set to be equal to the conductivity of air, while Figure 7*b* presents the contours produced by Bilgen [19], for the same setting. As can be seen in Figures 5–7 and Table 4, a very good agreement exists between the results obtained by our model when a partition is mounted and the results reported in previously published works.

Since the top and bottom walls are insulated, the average Nusselt number on the hot wall, defined in Eq. (8), must equal to the same quantity on the cold wall. This was verified for all the cases studied in this work.

6. RESULTS AND DISCUSSION

6.1. Vertical Partition on the Bottom Wall

When a vertical partition is attached, heat transfer is always smaller compared to an enclosure with no partitions, which leads to values of R_r smaller than one. Figure 8 demonstrates R_r variations with respect to Ra for $A = 1$ to $A = 4$ in an

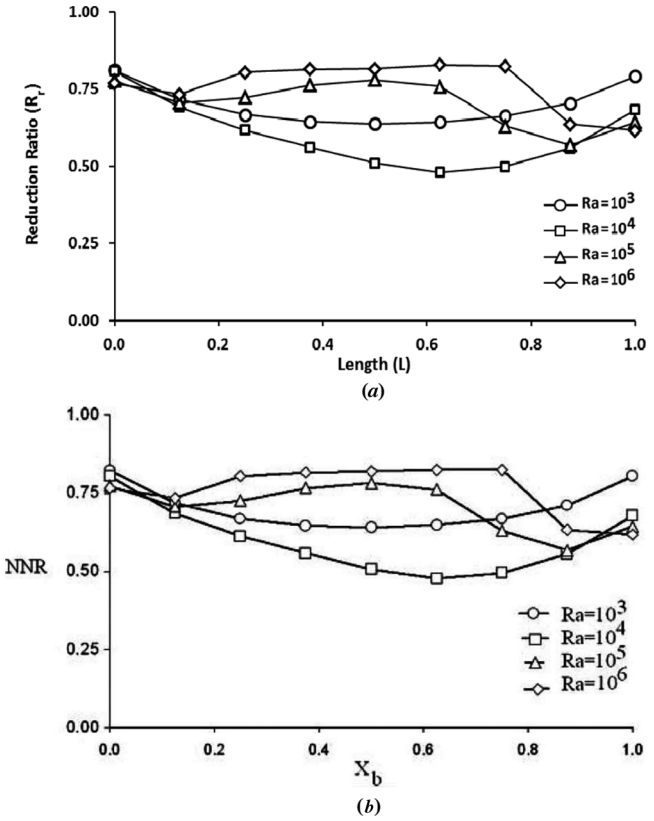

Figure 6. Reduction ratio with respect to the location of the vertical barrier for $L = 0.5$ at different Rayleigh numbers. (*a*) Present work, and (*b*) corresponding results from Ilis et al. [31].

enclosure with a vertical partition fixed on the bottom wall. It can be seen in Figures 8*a*–8*d* that for any A, the nondimensional length of the partition, L, has a significant effect on R_r; therefore, the curves corresponding to similar lengths are grouped together. Implementing longer vertical adiabatic baffles reduces the convection heat transfer, by more effectively disturbing the flow, as well as blocking a larger portion of conduction.

In the case of a square enclosure (Figure 8*a*) and at low Rayleigh numbers ($\mathrm{Ra} = 10^3$), 1-D conduction in the x direction is the dominant mode of heat transfer and the temperature gradient creates weak convection currents. When A and L are fixed and for $\mathrm{Ra} = 10^3$, changing the location of the partition would only disturb the minor buoyant flow and does not affect R_r considerably. Still, partitions located near the middle cause slightly lower R_r values. By increasing Ra convection plays an increasingly important role in the overall heat transfer of the system. Consequently, for fixed L, R_r gradually becomes more sensitive to D_x, and partitions block a larger portion of the overall heat transfer, leading to lower R_r minimums at 10^4. For a vertical partition of $L = 0.5$, minimum R_r occurs at $\mathrm{Ra} = 10^4$ and $D_x = 0.4$, yielding an R_r as small as 0.48, which is considerably smaller than the minimums for the same setting at other Rayleigh numbers. Since length is the most significant factor,

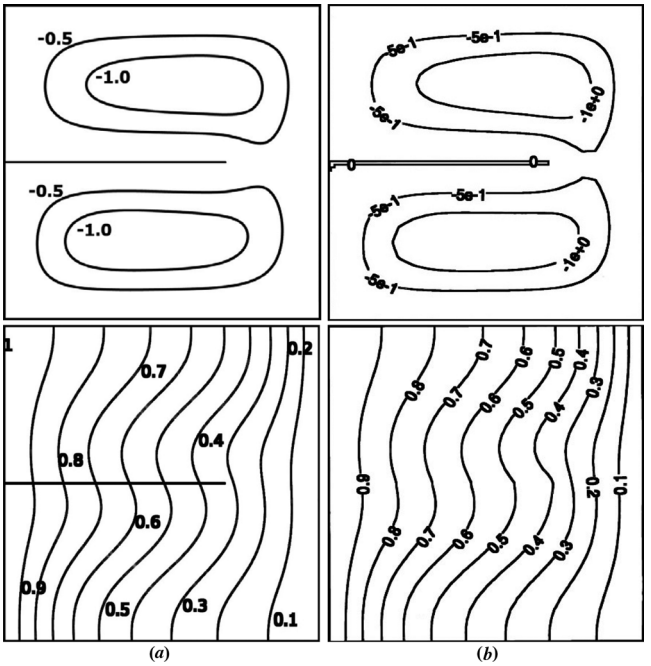

Figure 7. Streamlines and isotherms for $\mathrm{Ra} = 10^4$ in the presence of a horizontal partition fixed on the hot wall ($L = 0.7$, $D_y = 0.5$, and $k_p = k_{air}$). (*a*) Present work, and (*b*) results from Bilgen [19].

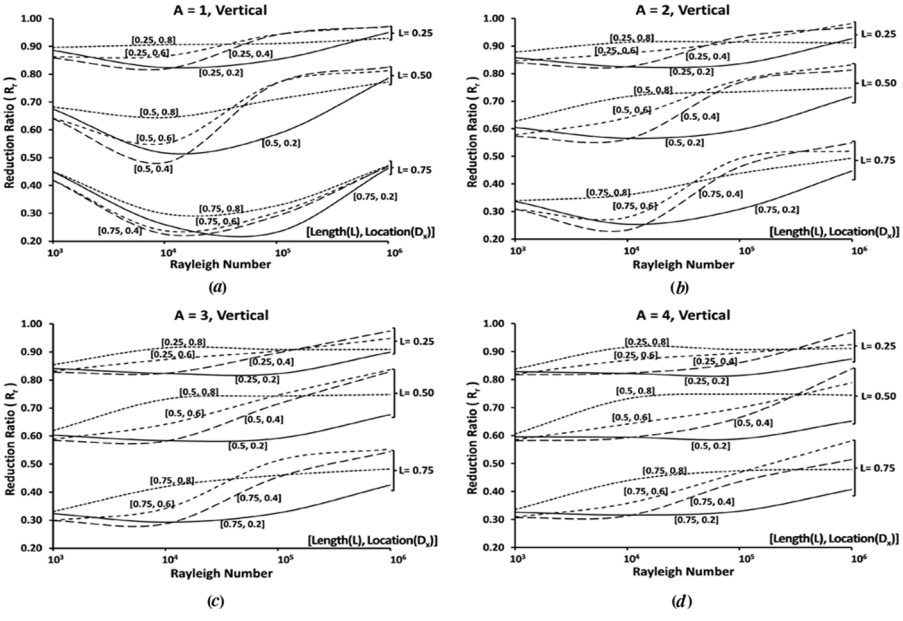

Figure 8. Reduction ratio variations with respect to Rayleigh number, length, and location in the presence of a vertical partition for (*a*) $A = 1$, (*b*) $A = 2$, (*c*) $A = 3$, and (*d*) $A = 4$.

a partition with $L = 0.75$ could result in an R_r value as low as 0.21. Figure 8*a* also reveals that by increasing Ra towards 10^6, generally, R_r increases, indicating a decrease in partition's effectiveness and R_r becomes less sensitive toD_x. Additionally, partitions with $D_x = 0.8$ (near the cold wall) begin to produce lower reduction ratios compared to other locations. In all three groups, at $\mathrm{Ra} = 10^3$, curves corresponding to $D_x = 0.4$ and $D_x = 0.6$ which have the same distance from the mid-plane, cross each other and yield the minimum R_r , indicating that the optimum position is close to the mid-plane. For $\mathrm{Ra} = 10^3$ to 10^4, R_r minimum occurs around $D_x = 0.4$ and for higher Rayleigh numbers ($\mathrm{Ra} = 10^4$ to $\mathrm{Ra} = 10^6$) the minimum R_r occurs around $D_x = 0.2$ and finally at $D_x = 0.8$. It can be concluded that by increasing the Rayleigh number, the D_x with minimum reduction is transferring from the center of the enclosure towards the hot wall.

Patterns associated with D_x in a square enclosure can be explained by considering the flow in an enclosure with no partitions. In the absence of obstacles and at low Rayleigh numbers the corners are relatively static regions due to the circular shape of the streamlines in the rectangular domain and an obstruction placed in these regions does not prominently redefine the flow. Instead streamlines are denser in the middle and as a result locations close to the mid-plane are optimum for heat transfer reduction. Figure 9*a*, demonstrates the flow fields generated by attaching a partition with $L = 0.5$ in the mid-plane of the bottom wall at different Rayleigh numbers for $A = 1$. At $\mathrm{Ra} = 10^3$, this figure illustrates how the vertical partition has affected the densely packed streamlines in the middle. By increasing *Ra*, this region of dense streamlines moves towards the hot wall and as can be seen in Figure 2, at $\mathrm{Ra} = 10^6$streamlines become tightly packed close to the enclosure corners in the absence of partitions. Therefore, the optimum D_x gradually decreases and a partition attached closer to the sidewalls disturb the flow more efficiently.

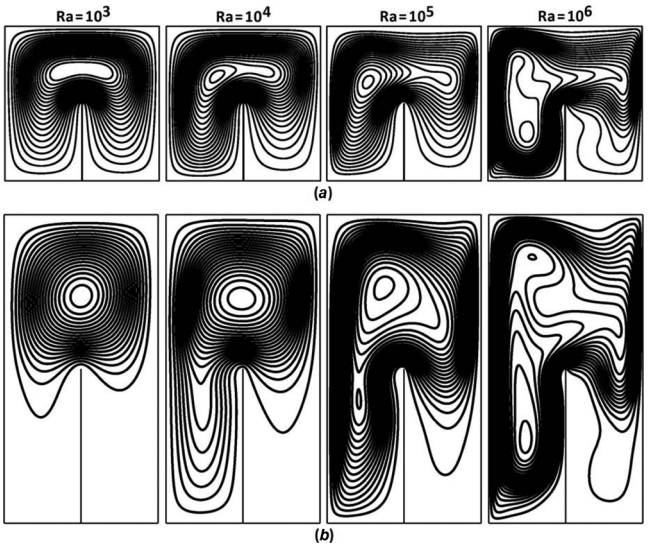

Figure 9. Streamlines at different Rayleigh numbers when a partition with $[L, D_x] = [0.5, 0.5]$ is mounted for (*a*) $A = 1$ and (*b*) $A = 2$.

Moreover, partitions close to the sidewalls also create relatively stationary regions between the partition and the sidewall, reducing the interaction between the fluid and the wall. This formation contributes to R_r reduction and is also mentioned by Ilis et al. [31]. For these reasons, locations close to the sidewalls are optimum at high Rayleigh numbers as high as 10^6. Figure 9*a* also demonstrates that by increasing Ra towards 10^6 the flow becomes stronger and a thin boundary layer is formed. This thin boundary layer encompasses tightly packed streamlines (with relatively large stream function values) which curve around the obstacle. As a result the boundary layer interacts with the active sidewalls regardless of the value of D_x. This is the reason for the overall decrease in partition's effectiveness and the steady increase of R_r as Ra increases, as seen in Figure 8*a*.

In taller enclosures (Figures 8*b*–8*d*), the effect of partitions on the conduction is similar to the square cavity case. Again, partition's length remains dominant and increasing L considerably reduces R_r in all situations. While all other parameters are fixed, increasing A leads to a small reduction in R_r at $\mathrm{Ra} = 10^3$. Specifically, this decline is considerable when increasing the aspect ratio from $A = 1$ to $A = 2$ and for longer partitions ($L = 0.5, 0.75$); at $\mathrm{Ra} = 10^3$ increasing the aspect ratio to $A = 2$ reduces R_r approximately by 8% for $L = 0.5$ and by 10% for $L = 0.75$. Conversely, increasing A leads to a minor increase in R_r for $\mathrm{Ra} = 10^4$ and 10^5. This increase in R_r is specifically considerable when shifting from $A = 1$ to $A = 2$, which is about 5–10% for $L = 0.5$ at $\mathrm{Ra} = 10^4$, and about 10–20% increase for $L = 0.75$ at $\mathrm{Ra} = 10^5$. Finally, changing A does not affect R_r at $\mathrm{Ra} = 10^6$. Because of these shifts, in Figures 8*b*–8*d* for fixed L and when the partition is fixed at the optimum location (D_x), R_r minimum values are almost equal for $10^3 < \mathrm{Ra} < 10^5$. Therefore, unlike when $A = 1$, the minimum R_r does not uniquely correspond to a specific Ra. For instance, for $A = 3$ and $L = 0.5$ at $\mathrm{Ra} = 10^3$, $D_x = 0.5$ leads to $R_{r,min} = 0.57$; while at $\mathrm{Ra} = 10^4$, $D_x = 0.4$ results in $R_{r,min} = 0.58$ and at $\mathrm{Ra} = 10^5$, $D_x = 0.2$ results in $R_{r,min} = 0.59$ which are all apart by only 0.02.

Different characteristics of square and higher aspect ratio enclosures at low Rayleigh numbers can be explained by noting how increasing the aspect ratio influences the flow inside the cavity. In taller enclosures, partitions with similar nondimensional lengths create narrower spaces between the partition and sidewalls compared to square enclosures. When Ra is small, it is harder for the flow to move in these narrower regions; therefore these relatively motionless areas start to play a more important role than in square cavities. At Ra numbers as low as 10^3, it is not possible for the flow to effectively penetrate into the narrow regions, which causes a large portion of the space surrounded in these regions to remain almost stationary with minimal heat interaction with the sidewalls. If the partition is located close to one of the side walls, only the space between the partition and that sidewall is almost stagnant. However, when the partition is located close to the middle, the regions between the partition and both sidewalls become relatively motionless and this effect intensifies. Figure 9*b*, demonstrates the flow fields generated by attaching a partition with $L = 0.5$in the mid-plane of the bottom wall at different Rayleigh numbers for $A = 2$. Figure 9*b* for $\mathrm{Ra} = 10^3$ illustrates that only a single minimally disturbed circular flow emerges in the space over the partition which is actively contributing to the overall heat transfer in the system and the lower portion has minimal impact on heat transfer. Therefore, the optimum position of the partition is in the mid-plane.

By gradually increasing Ra to 10^4 and 10^5, the streamlines tend to accumulate in a location left to the mid-plane, in absence of partitions. A partition located in these locations optimally pushes the circular stream upwards and yields minimum flow in both regions to the left and to the right of the partition. Consequently the optimum position shifts to locations to the left of the mid-plane, analogous to the square cavity case. Short partitions ($L = 0.25$) create gaps with considerably small height to width ratios, and this effect is almost insignificant. Therefore the curves corresponding to $L = 0.25$ are very similar in all four plots of Figure 8. As can be expected, longer partitions make the effect of narrow regions more intense and the length's impact is significant similar to the case of square enclosures.

Figure 9 illustrates that as Ra increases towards 10^6, more vigorous currents are generated, with the potential to infiltrate in the narrow gaps and actively interact with sidewalls. As a result, the partition's effectiveness decreases and R_r gradually increases in all the curves of Figures 8*a*–8*d*. Moreover, the effect of narrow regions becomes minimal and flow field's patterns become increasingly similar to the stretched version of the equivalent square setting; this can be observed by comparing Figures 9*a* and 9*b* for $\mathrm{Ra} = 10^6$. Consequently, as Ra increases towards 10^6, R_r values for$A > 1$ increase similar to the square cavity case. In the absence of partitions, at these high Rayleigh numbers, stronger boundary layer currents are tightly packed in the bottom corners, especially the left corner. Consequently, fixing a partition close to the left wall (hot wall) disturbs the flow most effectively and yields minimum R_r. As such, partitions with $D_x = 0.8$ (near the cold wall) begin to produce lower R_r compared to locations close to the mid-plane. At $\mathrm{Ra} = 10^6$, R_r is relatively more sensitive to D_x for $A > 1$ as compared to the $A = 1$ case, due to the narrow regions.

Figure 9 illustrates the disturbance of the main circulation pattern and its impact at different Ra numbers. In the first row ($A = 1$), the partition is disturbing the flow by convoluting the streamline patterns, resulting in a heat transfer reduction at lower Rayleigh numbers. As Ra increases, the stronger thin boundary layers become dominant. In the second row ($A = 2$) narrow regions are mainly responsible for the convection heat transfer reduction at lower Rayleigh numbers, and again the presence of a strong boundary layer attains dominance as the Rayleigh number increases. Similar patterns exist for a vertical partition attached on the upper wall, due to the symmetry considerations. For instance, in a square enclosure, increasing Ra would cause the location of the vertical partition on the ceiling with minimum R_r to move from the center towards the cold wall. This is evident in Figure 6 for the specific case of $L = 0.5$, and is also mentioned by Ilis et al. [31].

6.2. Horizontal Partition on the Hot Wall

Implementing a horizontal adiabatic partition on the vertical wall does not block conduction since its orientation is parallel to the conduction direction. Therefore, these partitions essentially modify the convection portion of the overall heat transfer. Figures 10 and 11 demonstrate R_r variations with respect to Ra for $A = 1$ to $A = 4$ in an enclosure with an adiabatic horizontal partition mounted on the hot wall. Since the length is not the dominant parameter in this case, the results could not be grouped based on L in a single eloquent plot, similar to vertical

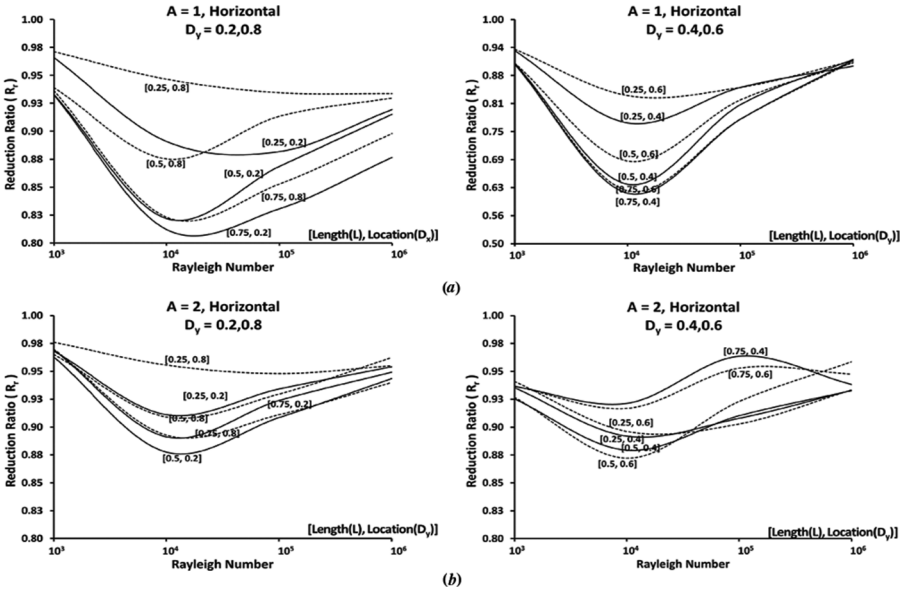

Figure 10. Reduction ratio variations with respect to Rayleigh number, length, and location in the presence of a horizontal partition for $D_y = 0.2,\ 0.8$(plots on the left), and $D_y = 0.4,\ 0.6$(plots on the right) for (a) $A = 1$ and (b) $A = 2$.

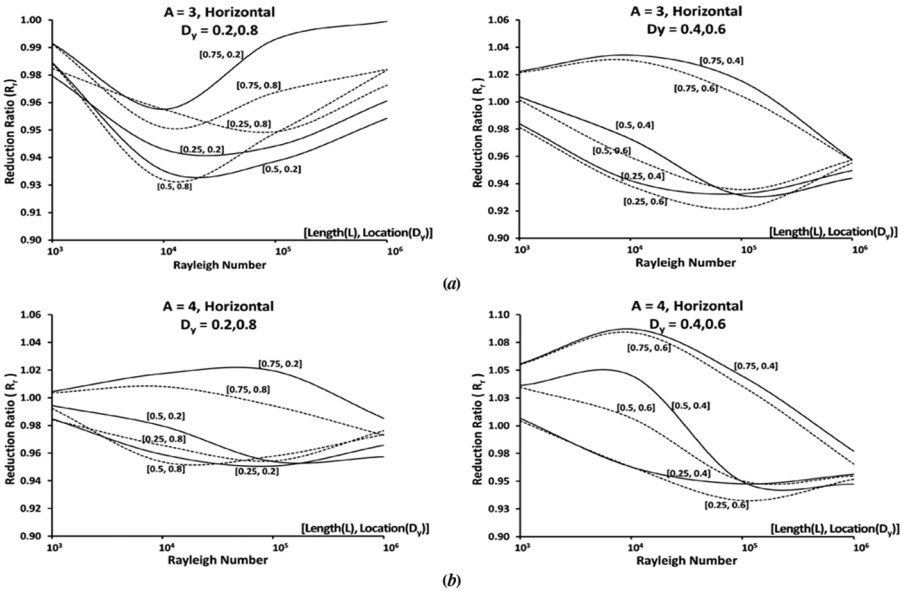

Figure 11. Reduction ratio variations with respect to Rayleigh number, length, and location in the presence of a horizontal partition for $D_y = 0.2,\ 0.8$ (plots on the left), and $D_y = 0.4,\ 0.6$ (plots on the right) for (a) $A = 3$ and (b) $A = 4$.

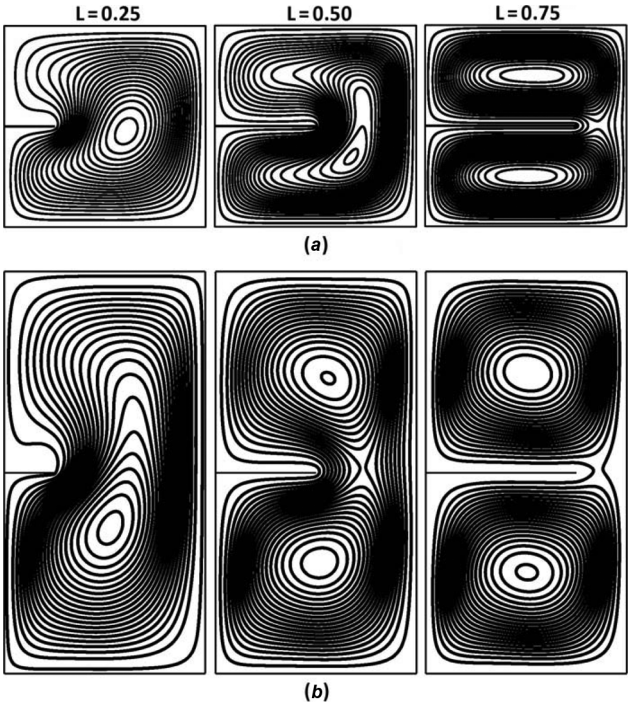

Figure 12. Streamlines at $\mathrm{Ra} = 10^4$ when a partition with $D_x = 0.5$ and different lengths is mounted for (*a*) $A = 1$ and (*b*) $A = 2$.

partitions. Therefore for each aspect ratio the results are divided and presented in two plots. Plots on the left are for cases with the partition located close to top and bottom walls and plots on the right are for cases with the partition located close to the mid-height.

For Rayleigh numbers close to 10^3, the convection contributes to a small portion of the overall heat transfer. Consequently, for horizontal partitions, when A is fixed and for $\mathrm{Ra} = 10^3$, changing the location or the length of the partition does not affect R_r significantly. Increasing Ra and implementing partitions with different L and D_y would produce an extended range of overall Nusselt reduction ratios.

In a square enclosure (Figure 10*a*), implementing a horizontal partition leads to reduction in heat transfer ($R_r < 1$). The decline in R_r is noticeable, though not as remarkable as a square cavity with a vertical partition. As expected, elongating the barrier makes it more efficient by more effectively disturbing the convective flow. This can be seen in Figure 12*a*, which demonstrates the flow fields generated by attaching a partition with different lengths in the mid-height of the hot wall cavity at $\mathrm{Ra} = 10^4$, for $A = 1$. Nevertheless unlike the vertical partitions, L is not the main dominant parameter; instead, D_y also plays an important role. Comparing the two plots of Figure 10*a* it is clear that for $\mathrm{Ra} > 10^3$ a horizontal partition located slightly below the mid-height ($D_y = 0.4$), is substantially more effective compared to a partition with the same length, located near the top and bottom walls. The reason

is that, as can be seen in Figure 2, streamlines are more packed in this area in the absence of partitions, and a partition in this area most effectively disturbs the flow as it can be seen in Figure 12. It is clear in Figure 10*a* that the lowest R_r values occur around $\mathrm{Ra} = 10^4$. Moreover, unlike an enclosure with a vertical partition, changing Ra does not influence the relative effectiveness of partitions with different lengths and locations as much, and for all Ra values there is a specific set of $[L, D_y]$ leading to the minimum R_r. For instance for a partition within a square enclosure with $L = 0.5$, the optimum position is $D_y = 0.4$ for all Ra values, yielding an R_r as low as 63% at $\mathrm{Ra} = 10^4$. Moreover, increasing Ra reduces the impact of both L and D_y, and around $\mathrm{Ra} = 10^6$ they become somewhat insignificant resulting in a small range of R_r for a square cavity with a horizontal partition.

The aspect ratio has a universal influence on the average R_r of the system, and higher A produces higher R_r values. In taller enclosures ($A > 1$), with a horizontal partition, R_r is greater than 0.88, therefore reduction ratios are not as significant as the case of a square enclosure. Moreover for $A > 2$, some cases even yield R_r values bigger than one, which indicates that the partition has caused an increase in the overall heat transfer of the system. This makes the implementation of a single horizontal partition quite inefficient in tall enclosures. The reason is that for $A > 1$, horizontal partitions would partially divide the chamber into two smaller domains, leading to development of two relatively separate vortices between the hot and the cold wall. This triggers an increasing effect on the overall heat transfer of the system which opposes the R_r reduction caused by baffles manipulating the flow field. The formation of these duplicate circulations is clear in Figure 12*b* which demonstrates the flow fields generated by attaching a partition with different lengths in the mid-height of the hot wall at $\mathrm{Ra} = 10^4$, for $A = 2$. Comparing Figures 12*a*, and 12b, shows that duplicate vortices are more prominent within taller cavities with horizontal partitions.

In Figs. 10b, 11, which correspond to cases that $A > 1$, R_r minimum occurs around Ra numbers between 10^4 and 10^5. As seen in Fig. 12*b*, longer partitions increase the probability of duplicate vortex formation. Therefore increasing length of the horizontal partition located close the mid-height can in fact augment the heat transfer after a certain point. As a result a partition with the same or higher length near the top or bottom wall can have an equivalent effectiveness. For instance, when $A = 2$ a partition with $[L, D_y] = [0.5, 0.6]$ or $[0.5, 0.4]$ would generate the minimum R_r at $Ra = 10^4$, equal to 0.87 or 0.88, respectively. A partition with the same length located close to the bottom ($D_y = 0.2$), would generate the same result ($R_r = 0.88$) at the same Rayleigh number. As such, for $A > 1$ the minimum R_r can be achieved by means of two options: First, implementing a baffle near the mid-plane where the vertical streamlines are dense, in order to disturb the flow, and at the same time implementing a partition short enough to avoid double vortex formation. As A increases, the maximum effective L corresponding to this option reduces, and D_y yielding minimum R_r gradually shifts from 0.4 to 0.6. Also, mounting a partition with the same or greater length near the top or bottom walls can take advantage of a larger interacting surface area without producing the double vortex formation. As Ra increases the optimum D_y corresponding to this option gradually shifts from 0.2 to 0.8. Based on our results, neither of these options is more effective than the other nor causes significant heat flux reduction.

For longer horizontal partitions located close to the middle of the chamber both vortices are fully developed. This can be seen for $L = 0.75$, in Fig. 12*b* at $Ra = 10^4$. Accordingly R_r values can become larger than one, as can be observed for some cases in Fig. 11. For instance for $A = 4$, $L = 0.75$ and $D_y = 0.4, 0.6$ results in an R_r which can be as high as 1.09, at $Ra = 10^4$. Similar analysis and conclusions could be drawn for a partition implemented on the cold wall, due to symmetry.

Based on our results, horizontal partitions on the sidewalls do not reduce the heat transfer as effectively as the vertical partitions on the top or bottom walls, with the exception of a few situations. In a square cavity ($A = 1$) at higher Rayleigh numbers ($Ra = 10^4, 10^5, 10^6$), short adiabatic horizontal partitions ($L = 0.25$) located near the mid-height ($D_y = 0.4, 0.6$) are 5–10% more effective than any vertical partition with the same non-dimensional length (L) fixed at any location (D_x), at the same Ra , due to more effective disturbance of convective currents. Nevertheless at $Ra = 10^3$ only the vertical adiabatic baffles can block the dominant conduction heat transfer and are more effective. Moreover in square enclosures, longer vertical adiabatic partitions ($L = 0.5, 0.75$) with the optimum D_x value (which is decreasing as Ra increases), are more effective at any Ra compared to equivalent horizontal partitions due to more effectively blocking both conduction and convection. In general, in higher aspect ratio enclosures narrow regions increase the effectiveness of vertical partitions while double vortex formations decrease the effectiveness of horizontal baffles. Thus, for any $A \geq 1$ and for any fixed Ra, a vertical partition with appropriate L and D_x would yield a lower R_r compared to a horizontal baffle with the same non-dimensional values of L and D_y.

6.3. Comprehensive Correlation

By interpolating the data gathered and the plots presented, the mean Nusselt number reduction ratio, R_r, can be estimated for the set of the input variables in the intervals investigated in this work. A statistical data set is generated based on the results gathered from the 384 simulations, and correlated by JMP software. A correlation for the mean Nusselt number reduction ratio, R_r, is obtained which incorporates the effects of the pertinent parameters such as the aspect ratio (A),

Table 5. Correlation coefficients for R_r in an enclosure with a vertical or a horizontal partition

Coefficient	Vertical	Horizontal
α_0	1.12515	0.80657
α_1	-6.4994×10^{-5}	4.0750×10^{-2}
α_2	−0.997501	1.3935×10^{-2}
α_3	0.109223	1.5518×10^{-2}
α_4	4.0349×10^{-7}	-1.0177×10^{-7}
α_5	-2.6166×10^{-3}	-1.1469×10^{-2}
α_6	−0.641952	0.193655
α_7	−0.201510	0.175580
α_8	−5.88625	2.34×10^{-13}
Average error	4.02%	3.28%

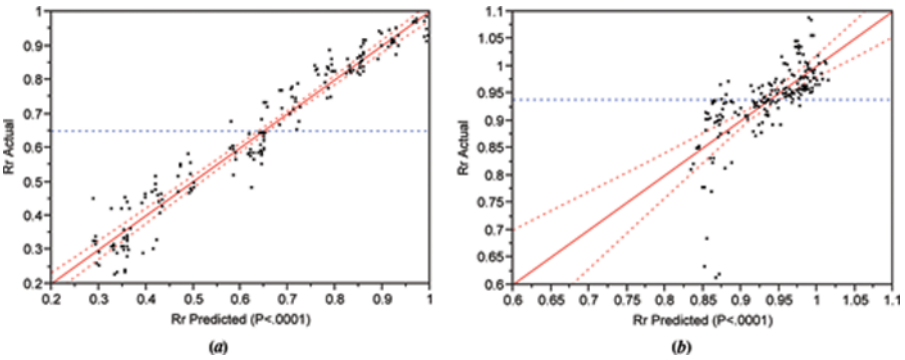

Figure 13. Actual mean Nusselt number reduction ratio versus that obtained from correlation Eq. (10) for (*a*) vertical partitions, and (*b*) horizontal partitions.

Rayleigh number (Ra), length (L), and location (D_x or D_y). This correlation is given in Eq. (10).

$$\begin{aligned} R_r = {} & \alpha_0 + \alpha_1 A + \alpha_2 L + \alpha_3 D_i + \alpha_4 \mathrm{Ra} \\ & + \alpha_5 (A - 2.5)^2 + \alpha_6 (L - 5)^2 \\ & + \alpha_7 (D_i - 5)^2 + \alpha_8 (\mathrm{Ra} - 277750)^2 \end{aligned} \tag{10}$$

In the above correlation, the subscript i stands for either x or y and α_0 to α_8 are the correlation coefficients. The values of the coefficients and the average associated errors for each case are presented in Table 5. This correlation covers both horizontal as well as vertical partitions studied in this work. Figure 13 shows the actual mean Nusselt number reduction ratio versus that obtained from the correlation, Eq. (10), for vertical and horizontal partitions. As can be seen, predicted and actual values match satisfactorily in most cases, which establishes good accuracy for the correlation expression introduced. There are only four points with noticeable residuals at the bottom of Figure 13*b* which correspond to cases with horizontal partitions of $L = 0.5, 0.75$ and $D_y = 0.4, 0.6$ at $\mathrm{Ra} = 10^3$. For these cases more accurate values of R_r can be obtained by means of the plots presented earlier.

7. CONCLUSIONS

Heat transfer reduction capability of a vertical or horizontal adiabatic partition fixed in a square or higher aspect ratio enclosures is studied, taking into account the effect of its length and location. Based on our results:

1. Vertical adiabatic partitions cause heat transfer suppression through the cavity while horizontal adiabatic partitions can increase the overall heat transfer, especially with higher values of length and in higher aspect ratio enclosures.
2. For vertical partitions, length is clearly the dominant factor, with longer partitions causing lower heat transfer rates; while for horizontal partitions both length and location play important roles, with regards to heat transfer reduction.

3. For vertical partitions in square cavities and for horizontal partitions in enclosures of different aspect ratios, first sensitivity of R_r to length and location augments, as Ra increases from 10^3 and then degrades as Ra further increases towards 10^6.
4. For heat reduction purposes, at Rayleigh numbers as small as 10^3 the optimum location for a vertical partition, is around the middle of upper or lower horizontal walls. As the Rayleigh number increases, regions close to sidewalls become progressively more favorable.
5. At low Rayleigh numbers, as the aspect ratio increases, vertical partitions more effectively reduce heat transfer due to formation of relatively motionless regions, and horizontal partitions become less effective (almost insignificant) due to increased potential for double vortex formation. As Ra increases, the effectiveness of both vertical and horizontal baffles becomes similar to their counterpart in square enclosures. The reason is formation of active cells within the regions separated by the baffles.
6. In general, a partition can more effectively reduce heat transfer when it is vertically fixed on the top or bottom wall; except for a shorter horizontal partition, which can cause slightly more heat transfer reduction when located close to the mid-height of a square cavity as compared to an equivalent vertical case.

REFERENCES

1. I. Catton, Natural Convection in Enclosures, *Proc. 6th Int. Heat Transfer Conf.,* Toronto, Canada, vol. 6, pp. 13–43, 1978.
2. S. Ostrach, Natural Convection in Enclosures, *J. Heat Transfer*, vol. 110, pp. 1175–1190, 1988.
3. Y. Jaluria, *Natural Convection Heat and Mass Transfer*, Pergamon Press, Oxford, UK, pp. 209–235, 1980.
4. E. M. Del Campo, M. Sen, and E. Ramos, Analysis of Laminar Convection in a Triangular Enclosure, *Numer. Heat Transfer* A, vol. 13, pp. 353–372, 1988.
5. M. Corcione, Effects of the Thermal Boundary Conditions at the Sidewalls upon Natural Convection in Rectangular Enclosures Heated from Below and Cooled from Above, *Int. J. Thermal Sci.*, vol. 42, pp. 199–208, 2003.
6. A. Dalal and M. K. Das, Natural Convection in a Rectangular Cavity Heated from Below and Uniformly Cooled from the Top and Both Sides, *Numer. Heat Transfer A*, vol. 49, pp. 301–322, 2006.
7. A. Bahlaoui, A. Raji, R. El Ayachi, M. Hasnaoui, M. Lamsaadi, and M. Naimi. Coupled Natural Convection and Radiation in a Horizontal Rectangular Enclosure Discretely Heated from Below, *Numer. Heat Transfer A*, vol. 52, pp. 1027–1042, 2007.
8. R. L. Frederick, Heat Transfer Enhancement in Cubical Enclosures with Vertical Fins, *Appl. Therm. Eng.* pp. 1585–1592, 2007.
9. Y. Varol, H. F. Öztop, F. Özgen, and A. Koca, Experimental and Numerical Study on Laminar Natural Convection in a Cavity Heated from Bottom due to an Inclined Fin, *Heat Mass Transfer*, vol. 48, pp. 61–70, 2012.
10. S. Jani, M. Mahmoodi, M. Amini, and J. E. Jam, Numerical Investigation of Natural Convection Heat Transfer in a Symmetrically Cooled Square Cavity with a Thin Fin on its Bottom Wall, *Therm. Sci.*, no. 00, pp. 139–139, 2012.

11. K. Hanjalic, S. Kenjeres, and F. Durst, Natural Convection in Partitioned Two-Dimensional Enclosures at Higher Rayleigh Numbers, *Int. J. Heat Mass Transfer*, vol. 39, pp. 1407–1427, 1996.
12. E. Zimmerman, and S. Acharya, Natural Convection in an Enclosure with a Vertical Baffle, *Comm. Appl. Numer. M.*, vol. 4, pp. 631–638, 1988.
13. R. L. Frederick and A. Valencia, Heat Transfer in a Square Cavity with a Conducting Partition on its Hot Wall, *Int. Comm. Heat Mass Transfer*, vol. 16, pp. 347–354, 1989.
14. S. Acharya and R. Jetli, Heat Transfer due to Buoyancy in a Partially Divided Square Box, *Int. J. Heat Mass Transfer*, vol. 33, pp. 931–942, 1990.
15. K. S. Chen and P. W. Ko., Natural Convection in a Partially Divided Rectangular Enclosure with an Opening in the Partition Plate and Isoflux Side Walls, *Int. J. Heat Mass Transfer*, vol. 34, pp. 237–246, 1991.
16. A. Nag, A. Sarkar, and V. M. K. Sastri, Natural Convection in a Differentially Heated Square Cavity with a Horizontal Partition Plate on the Hot Wall, *Comput. Meth. Appl. Mech. Eng.*, vol. 110, pp. 143–156, 1993.
17. X. Shi and J. M. Khodadadi, Laminar Convection Heat Transfer in a Differentially Heated Square Cavity due to a Thin Fin on the Hot Wall, *J. Heat Transfer*, vol. 125, pp. 624–634, 2003.
18. S. H. Tasnim and M. R. Collins, Numerical Analysis of Heat Transfer in a Square Cavity with a Baffle on the Hot Wall, *Int. Comm. Heat Mass Transfer*, vol. 31, pp. 639–650, 2004.
19. E. Bilgen, Natural Convection in Cavities with a Thin Fin on the Hot Wall, *Int. J. Heat Mass Transfer*, vol. 48, pp. 3493–3505, 2005.
20. P. Oosthuizen and J. T. Paul, Free Convection Heat Transfer in a Cavity Fitted with a Horizontal Plate on the Cold Wall, Advances in Enhanced Heat Transfer—1985, Presented at the *23rd ASME National Heat Transfer Conf.*, vol. 43, pp. 101–107, 1985.
21. R. Scozia and R. L. Frederick, Natural Convection in Slender Cavities with Multiple Fins Attached on an Active Wall, *Numer. Heat Transfer A*, vol. 20, pp. 127–158, 1991.
22. G. N. Facas, Natural Convection in a Cavity with Fins Attached to Both Vertical Walls, *J. Thermophys. Heat Transfer*, vol. 7, pp. 555–560, 1993.
23. R. L. Frederick and A. Valencia, Natural Convection in Central Microcavities of Vertical, Finned Enclosures of Very High Aspect Ratios, *Int. J. Heat Fluid Flow*, vol. 16, pp. 114–124, 1995.
24. V. I. Terekhov and V. V. Terekhov, Heat Transfer in a High Vertical Enclosure with Fins Attached to one of the side walls, *High Temp.*, vol. 44, pp. 436–441, 2006.
25. V. I. Terekhov and V. V. Terekhov, Heat Transfer in a High Vertical Enclosure with Multiple Fins Attached to the Wall, *J. Enhanced Heat Transfer*, vol. 15, no. 4, pp. 303–312, 2008.
26. E. Bilgen, Natural Convection in Enclosures with Partial Partitions, *Renewable Energy*, vol. 26, pp. 257–270, 2002.
27. E. S. Nowak and M. H. Novak, Vertical Partitions in Slender Rectangular cavities, *Int. J. Heat Fluid Flow*, vol. 15, no. 2, pp. 104–110, 1994.
28. S. Oztuna, A Differential Quadrature Solution of Natural Convection in an Enclosure with a Partial Partition, *Numer. Heat Transfer A*, vol. 52, pp. 1009–1026, 2007.
29. M. Ciofalo and T. G. Karayiannis, Natural Convection Heat Transfer in a Partially—or Completely—Partitioned Vertical Rectangular Enclosure, *Int. J. Heat Mass Transfer*, vol. 34, pp. 167–179, 1991.
30. M. W. Nansteel and R. Greif, Natural convection in Undivided and Partially Divided Rectangular Enclosures, *J. of Heat Transfer*, vol. 103, pp. 623–629, 1981.
31. G. G. Ilis, M. Mobedi and H. F. Öztop, Heat Transfer Reduction due to a Ceiling-Mounted Barrier in an Enclosure with Natural Convection, *Heat Transfer Eng.*, vol. 32, no. 5, 429–438, 2011.

32. D. de Vahl Davis, Natural Convection of Air in a Square Cavity: A Bench Mark Solution, *Int. J. Numer. Meth. Fluids*, vol. 3, pp. 249–264, 1983.
33. G. Barakos, E. Mitsoulis, and D. Assimacopoulos, Natural Convection Flow in a Square Cavity Revisited: Laminar and Turbulent Models with Wall Functions, *Int. J. Numer. Meth. Fluids*, vol. 18, pp. 695–719, 1994.
34. N. C. Markatos and K. A. Pericleous, Laminar and Turbulent Natural Convection in an Enclosed Cavity, *Int. J. of Heat and Mass Transfer*, vol. 27, pp. 755–772, 1984.
35. T. Fusegi, J. M. Hyun, K. Kuwahara, and B. Farouk, A Numerical Study of Three-Dimensional Natural Convection in a Differentially Heated Cubical Enclosure, *Int. J. Heat Mass Transfer*, vol. 34, pp. 1543–1557, 1991.